Available online at www.sciencedirect.com

ScienceDirect

Procedia Structural Integrity 37 (2022) 788–795

Structural Integrity Procedia

www.elsevier.com/locate/procedia

ICSI 2021 The 4th International Conference on Structural Integrity

Accuracy of models of concrete in circular columns using different proposals for the prediction of failure of the confining FRP

Paulo Silva Lobo[a,b], Mariana Jesus[a,c,*]

[a]CERIS, Instituto Superior Técnico, Universidade de Lisboa, Av. Rovisco Pais 1, 1049-001 Lisboa, Portugal
[b]Departamento de Engenharia Civil e Geologia, Faculdade de Ciências Exatas e da Engenharia, Universidade da Madeira, Campus Universitário da Penteada, 9020-105 Funchal, Portugal
[c]DEC, NOVA School of Science and Technology, Universidade Nova de Lisboa, 2829-516 Caparica, Portugal

Abstract

Confinement of concrete columns with fiber reinforced polymers results in an increase of strength and ductility. For this reason, the use of aramid, carbon and glass-based composites for confinement of reinforced concrete columns has significantly increased over the last decades. Nevertheless, few models adequately predict the failure strain of the fiber reinforced polymer, which has a determinant influence on the computed results. In this paper the accuracy of existing models of confined concrete using different proposals for the prediction of the failure strain of the confining composite is assessed. This is based on the comparison of analytical results with experimental test results of concrete columns with circular cross-section reported in the literature. The comparison focusses on different parameters such as strength, maximum strain and strain energy density.

Keywords: Fiber Reinforced Polymers ; Failure Strain ; Concrete Confinement

1. Introduction

The confinement with externally applied fiber reinforced polymers (FRP) results in notorious improvement of ductility and strength. For this reason, the use of FRP-based composites for the confinement of reinforced concrete columns has significantly increased over the last decades. Confinement has been studied with great emphasis in recent years, particularly regarding the behaviour of reinforced concrete columns confined with aramid fiber reinforced polymers (AFRP), carbon fiber reinforced polymers (CFRP) and glass fiber reinforced polymers (GFRP) sheets.

The first studies regarding confinement of columns were presented by Richard and Abbott (1975) and Mander et al. (1988), who proposed the first equations to compute the maximum strength, the axial strain and the behaviour of FRP confined columns. In the following studies FRP models were categorized in two main groups, namely theoretical

* Corresponding author.
E-mail address: mc.jesus@campus.fct.unl.pt

10.1016/j.prostr.2022.02.010

models, based on physical concepts, that use an incremental numeric procedure to obtain stress-strain curves, and, design-oriented models, obtained through calibration of the parameters that influence the stress-strain curve, using experimental results. Numerical implementation of theoretical models is usually more complex, making it possible to determine the stress-strain curve until failure of the FRP, while design-oriented models are easier to implement, resulting in adequate predictions of strength and ultimate strain of confined concrete columns.

The theoretical model proposed by Spoelstra and Monti (1999) for monotonic loading of concrete columns confined with FRP describes the stress-strain relationship based on the equation by Popovics (1973), which considers the increase of the lateral confining pressure with the increase of the axial load, being the maximum confining stress obtained through an equation proposed by Mander et al. (1988).

The design-oriented models by Chastre and Silva (2010) for CFRP, by Jesus et al. (2018) for GFRP and by Silva Lobo et al. (2018) for AFRP are based on a constitutive model for circular columns based on the stress-strain relationship by Richard and Abbott (1975). For each of these models, the authors calibrated the required parameters mainly based on experimental results found in the literature. Also, the peak strength is obtained through the equation proposed by Mander et al. (1988). Regarding the design-oriented models by Lam and Teng (2003a) and by Wei and Wu (2012) for FRP, only the stress-axial strain relationship was proposed, and in both models the peak stress is based on the equation proposed by Mander et al. (1988). The stress-axial strain relationship of the model by Lam and Teng (2003a) was obtained through calibration of the parameters of the model by Spoelstra and Monti (1999), and the stress-axial strain relationship of the model by Wei and Wu (2012) was obtained through calibration of the parameters of the models by Lam and Teng (2003a,b, 2004).

In the present work, the accuracy of both theoretical and design-oriented models were assessed with different proposals for the prediction of failure of the FRP.

2. Experimental tests from the literature

The experimental results of circular columns confined with AFRP chosen for comparison with results obtained with the mentioned numerical models are from Dai et al. (2011) (AT2, a set of three equal specimens with the same characteristics), Wu et al. (2008) (AF2) , Silva Lobo et al. (2018) (AC) and Vincent and Ozbakkaloglu (2013) (NWE90, a set of three equal specimens with the same characteristics). For CFRP, the experimental results considered are from Toutanji (1999) (C1 and C5) and Berthet et al. (2005). Regarding GFRP, the experimental tests considered are those by Toutanji (1999) (GE), Lam and Teng (2004) (G1 and G2, a set of two equal specimens with the same characteristics) and Silva and Chastre (2006) (EE75C). The main properties of the specimens considered can be found in Table 1.

Table 1. Experimental results

Author	Specimen	Geometry	FRP Properties						Concrete Properties			
		D [mm]	type	no. layers	t_j [mm]	E_j [GPa]	ε_{ju} [%]	ε_{lu} [%]	f_{co} [MPa]	ε_{co} [%]	f_{cc} [MPa]	ε_{cc} [%]
Wu et al. (2008)	AF2	150	AFRP	1	0.29	115	2.0	2.5	23.1	0.27	50.7	3.03
Dai et al. (2011)	AT2	150	AFRP	2	0.17	115	3.2	3.0	39.2	0.33	88.9	3.45
Vincent and Ozbakkaloglu (2013)	NWE90	150	AFRP	3	0.20	116	2.5	2.2	49.4	0.24	106.2	3.02
Silva Lobo et al. (2018)	AC	200	AFRP	1	0.20	120	2.3	2.3	18.9	0.49	36.9	2.73
Toutanji (1999)	C1	76	CFRP	2	0.11	231	1.5	1.3	30.9	0.19	95.0	2.45
Toutanji (1999)	C5	76	CFRP	2	0.17	373	0.8	0.6	30.9	0.19	94.0	1.55
Berthet et al. (2005)	C20C1	160	CFRP	1	0.17	230	1.4	1.0	25.0	0.23	42.8	1.63
Berthet et al. (2005)	C20C2	160	CFRP	2	0.17	230	1.4	0.9	25.0	0.23	55.2	1.73
Toutanji (1999)	GE	76	GFRP	2	0.12	73	2.1	1.6	29.9	0.19	60.8	1.53
Lam and Teng (2004)	G1	152	GFRP	1	1.27	22	1.6	1.5	38.5	0.20	55.1	1.39
Lam and Teng (2004)	G2	152	GFRP	2	1.27	22	1.6	1.6	38.5	0.20	76.5	2.33
Silva and Chastre (2006)	EE75C	250	GFRP	2	1.27	21	2.2	0.6	26.5	0.19	55.8	1.10

D is the diameter of the cross-section, *no. layers* is a reference to the number of layers of FRP used, t_j is the design thickness of one FRP sheet, E_j is the Young's modulus of the FRP, ε_{ju} is the ultimate strain provided by the manufacturer, ε_{lu} is the observed experimental failure strain, f_{co} is the unconfined concrete strength, ε_{co} is the strain corresponding to f_{co}, f_{cc} is the peak strength and ε_{cc} is the strain corresponding to f_{cc}.

3. Comparison of numerical and experimental results

The accuracy of models of confined concrete using different proposals for the prediction of the failure strain of the confining composite is assessed herein. The comparison between numerical results and experimental tests focus on the analysis of different parameters such as f_{cc}, ε_{cc} and strain energy density (W) for all three FRP.

Each model was combined with the equations for the prediction of the FRP lateral failure strain found in literature, presented in Table 2.

Table 2. Equations of ε_{lu} / ε_{ju} for columns with circular cross-section.

Author	$\varepsilon_{lu}/\varepsilon_{ju}$		Note:
Arabshahi et al. (2020)	$0.83 - 2 \times \frac{f_{co}}{E_j}$	(1)	for AFRP
Benzaid et al. (2010)	0.73	(2)	for CFRP
Ilky et al. (2004)	0.79	(3)	for CFRP
Lam and Teng (2003a)	0.586	(4)	for CFRP
	0.788		for HM CFRP
	0.851		for AFRP
	0.624		for GFRP
	0.632		for FRP
Manfredi and Realfonzo (2001)	0.685	(5)	for FRP
Matthys et al. (2005)	0.60	(6)	for CFRP and GFRP
Ozbakkaloglu and Lim (2013)	$0.9 - 0.75 \times \frac{E_j}{10^6} - 2.3 \times \frac{f_{co}}{10^3}$	(7)	for FRP
Silva Lobo et al. (2018)	0.85	(8)	for AFRP
Toutanji et al. (2010)	0.43	(9)	for FRP
Vincent and Ozbakkaloglu (2013)	0.737	(10)	for NSC and CFRP
	0.656		for HSC and CFRP
	0.548		for UHSC and CFRP

The error of each numerical models compared to the experimental results, regarding f_{cc} and ε_{cc}, for columns with circular cross-section confined with AFRP is presented in Table 3. The error, in general, can be obtained by

$$error\ (\%) = \frac{t_v - n_v}{t_v} \times 100 \tag{1}$$

were t_v is the value of the experimental test and n_V is the value of the numerical model.

Table 3. Error of model predictions compared to experimental results for columns confined with AFRP.

		Equation (1)		Equation (4)		Equation (5)		Equation (7)		Equation (8)		Equation (9)	
Specimen	Model	f_{cc}	ε_{cc}	f_{cc}	ε_{cc}	f_{cc}	ε_{cc}	f_{cc}	ε_{cc}	f_{cc}	ε_{cc}	f_{cc}	ε_{cc}
AC	Spoelstra and Monti (1999)	-9.89	-170.70	-11.13	-182.42	-3.03	-112.09	-12.74	-198.17	-11.09	-182.05	11.81	-16.12
	Lam and Teng (2003a)	4.54	-38.83	3.09	-43.96	12.00	-13.55	1.18	-50.55	3.14	-43.59	25.67	26.74
	Wei and Wu (2012)	16.79	-35.90	15.81	-38.46	21.88	-22.34	14.51	-41.76	15.85	-38.46	31.40	4.40
	Silva Lobo et al. (2018)	-3.20	-3.30	-4.20	-6.59	2.14	13.92	-5.51	-10.99	-4.17	-6.59	12.84	45.42
AF2	Spoelstra and Monti (1999)	-2.05	-74.92	-3.32	-83.50	3.97	-38.28	-4.68	-93.07	-3.27	-83.17	17.56	23.43
	Lam and Teng (2003a)	-3.35	-17.82	-5.49	-23.43	6.20	5.61	-7.96	-30.03	-5.41	-23.43	24.16	44.22
	Wei and Wu (2012)	21.05	32.01	19.89	30.69	26.27	38.61	18.56	29.04	19.93	30.69	36.25	52.15
	Silva Lobo et al. (2018)	-5.78	-11.22	-7.05	-15.51	-0.02	6.93	-8.51	-20.13	-7.01	-15.18	11.33	41.25
AT2	Spoelstra and Monti (1999)	-1.16	-138.03	-3.10	-156.56	4.02	-93.73	-4.34	-169.02	-3.07	-156.27	17.62	-6.56
	Lam and Teng (2003a)	17.27	14.58	14.98	8.78	22.96	28.76	13.48	4.73	15.03	8.78	35.23	55.69
	Wei and Wu (2012)	20.26	39.48	18.28	37.74	25.22	44.40	16.98	36.29	18.33	37.74	36.10	55.98
	Silva Lobo et al. (2018)	7.90	18.05	6.35	13.42	11.86	29.92	5.35	10.23	6.38	13.42	21.10	55.41
NWE90	Spoelstra and Monti (1999)	-9.40	-59.20	-12.01	-75.12	-4.70	-33.67	-13.19	-82.75	-12.01	-75.12	9.76	24.71
	Lam and Teng (2003a)	-3.30	-5.14	-7.85	-15.75	4.11	11.77	-9.94	-20.73	-7.78	-15.75	22.49	48.26
	Wei and Wu (2012)	13.29	52.90	10.28	50.91	18.26	56.22	8.92	49.92	10.33	50.91	30.74	64.84
	Silva Lobo et al. (2018)	-7.13	-7.79	-9.84	-16.42	-2.68	5.80	-11.05	-20.40	-9.81	-16.42	8.90	39.97

The stress-strain curves for columns confined with AFRP were analysed for the models with lower error values of f_{cc} and ε_{cc} (see Fig. 1). The comparison of the W of the models with the W of the experimental test, for the smaller error value of f_{cc} and ε_{cc}, are presented in Table 4.

Regarding the specimen AC, the stress-axial strain curve and the stress-lateral strain curve of the model by Silva Lobo et al. (2018) coupled with equations (1) and (7) presents a similar behaviour and almost coincident with the

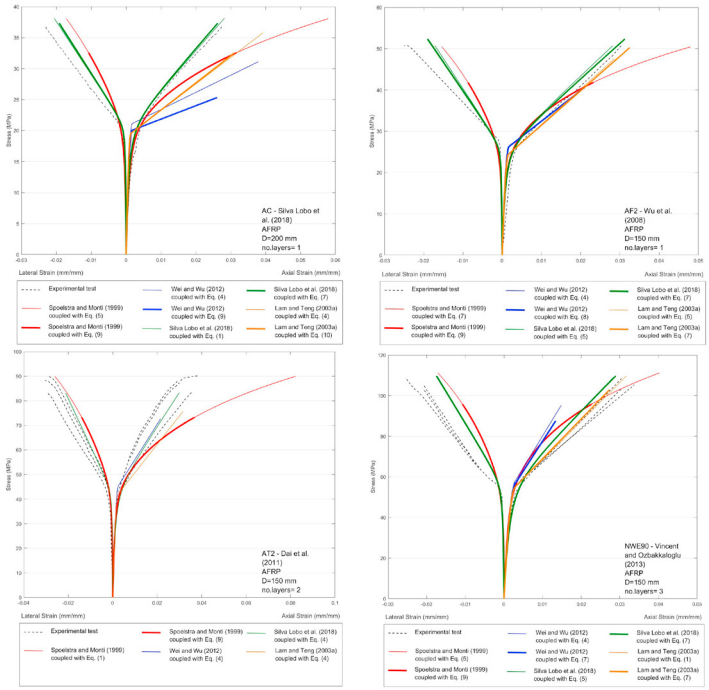

Fig. 1. Comparison of numerical stress-strain curves with experimental data for columns confined with AFRP.

Table 4. Error of the strain energy density prediction for specimens confined with AFRP.

Model	AC		AF2		AT2		NWE90	
	Equation	W	Equation	W	Equation	W	Equation	W
Spoelstra and Monti (1999)	(5)	-139.28	(7)	16.16	(1)	-198.28	(5)	-52.97
	(9)	-13.06	(9)	66.29	(9)	-9.33	(9)	26.35
Lam and Teng (2003a)	(4)	-44.66	(5)	56.62	(4)	10.12	(1)	-7.08
	(5)	-6.95	(7)	48.71			(7)	11.94
Wei and Wu (2012)	(4)	-31.14	(4)	70.43	(4)	39.55	(4)	55.76
	(9)	21.76	(8)	70.87			(7)	62.68
Silva Lobo et al. (2018)	(1)	-8.10	(5)	54.72	(4)	9.20	(5)	4.69
	(7)	1.06	(7)	48.48			(7)	2.23

behaviour of specimen AC. When analysing the error of W for specimen AC, it is possible to confirm that the model with less error is the model by Silva Lobo et al. (2018) coupled with equation (7). For specimen AF2, regarding the stress-axial strain curves, the model by Spoelstra and Monti (1999) and by Lam and Teng (2003a), both coupled with equations (5) and (7), presents the most representative behaviour of the specimen. Regarding the stress-lateral strain curves, no model were representative of the behaviour of the specimen. When analysing the error of W for specimen AF2, it is noted that the errors are very high (> 48%), with exception of the error value by the model of Spoelstra and Monti (1999) coupled with equation (7).

Regarding the specimen AT2, the stress-axial strain behaviour of all models coupled with equation (4), with exception of the model by Spoelstra and Monti (1999) are closest to the curves of the specimen AT2. For the stress-lateral strain curves, it is noted that both models by Spoelstra and Monti (1999), coupled with equations (1) and (9), and by Silva Lobo et al. (2018) coupled equation (4) are representative of the behaviour of the specimen. The errors of W are small for the models by Spoelstra and Monti (1999) coupled with equation (9) and the model by Silva Lobo et al. (2018) coupled with equation (4). For specimen NWE90, the stress-axial strain curve of the model by Lam and Teng (2003a) coupled with equations (1) and (7) is coincident with the experimental results. The stress-lateral strain behaviour of the experimental test is not represented by any of the models. Regarding the errors of W, the model by Silva Lobo et al. (2018) coupled with equation (7) presents the smaller value of error.

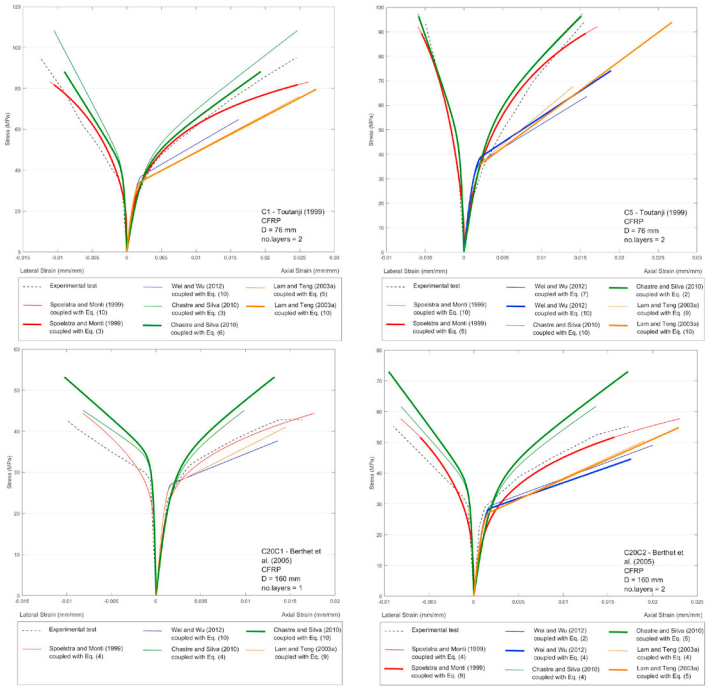

Fig. 2. Comparison of the numerical stress-strain curves with the experimental data for columns confined with CFRP.

The error between numerical models and experimental tests, regarding f_{cc} and ε_{cc}, for columns with circular cross-section confined with CFRP are presented in Table 5.

Table 5. Error of model predictions compared to experimental results for columns confined with CFRP

Specimen	Model	Equation (2)		Equation (3)		Equation (4)		Equation (5)		Equation (6)		Equation (7)		Equation (9)		Equation (10)	
		f_{cc}	ε_{cc}	f_{cc}	ε_{cc}	f_{cc}	ε_{cc}	f_{cc}	ε_{cc}	f_{cc}	ε_{cc}	f_{cc}	ε_{cc}	f_{cc}	ε_{cc}	f_{cc}	ε_{cc}
C1	Spoelstra and Monti (1999)	12.73	-6.12	13.94	-0.82	18.90	18.37	14.52	1.63	18.20	15.92	7.58	-32.24	27.48	43.67	12.46	-7.35
	Lam and Teng (2003a)	16.73	-10.20	18.83	-4.49	26.75	15.92	19.88	-1.63	25.78	13.47	6.61	-39.59	37.59	41.63	16.25	-11.84
	Chastre and Silva (2010)	-21.06	-7.76	-13.99	-0.82	9.89	23.67	-10.56	2.86	7.19	20.82	-60.02	-43.67	35.17	51.84	-22.72	-8.98
	Wei and Wu (2012)	32.11	34.29	33.47	35.92	38.70	42.45	34.15	36.73	38.07	41.63	25.51	26.53	45.98	51.43	31.79	34.29
C5	Spoelstra and Monti (1999)	2.38	-9.68	4.10	-3.87	10.66	15.48	4.89	-1.29	9.70	12.90	-3.73	-33.55	22.23	41.29	2.01	-10.97
	Lam and Teng (2003a)	0.77	-70.32	3.50	-61.94	13.86	-29.68	4.86	-57.42	12.61	-33.55	-11.49	-112.26	28.05	9.03	0.14	-72.90
	Chastre and Silva (2010)	-2.45	2.58	2.89	9.03	21.03	30.32	5.45	11.61	18.93	27.74	-29.24	-27.10	40.42	53.55	-3.64	1.29
	Wei and Wu (2012)	21.58	-21.29	23.34	-18.06	30.07	-6.45	24.22	-16.77	29.25	-7.74	13.71	-34.84	39.43	11.61	21.17	-21.94
C20C1	Spoelstra and Monti (1999)	-10.99	-41.46	-9.48	-34.11	-3.66	-8.39	-8.70	-30.43	-4.40	-11.45	-17.58	-76.97	5.48	24.68	-11.24	-42.68
	Lam and Teng (2003a)	4.48	11.82	6.00	15.49	11.81	28.97	6.79	17.33	11.10	27.74	-2.99	-7.16	19.73	46.11	4.14	11.21
	Chastre and Silva (2010)	-23.28	19.78	-19.22	24.68	-5.27	39.99	-17.21	26.52	-6.88	38.15	-46.22	-4.72	9.54	55.30	-24.29	19.17
	Wei and Wu (2012)	12.26	17.33	13.39	19.17	17.73	25.90	13.97	19.78	17.20	25.29	6.73	8.76	23.76	36.31	11.99	16.72
C20C2	Spoelstra and Monti (1999)	-12.64	-75.07	-10.99	-65.80	-4.49	-33.33	-10.24	-61.74	-5.25	-36.81	-19.69	-120.29	6.40	8.99	-12.94	-76.81
	Lam and Teng (2003a)	4.48	11.82	6.00	15.49	11.81	28.97	6.79	17.33	11.10	27.74	-2.99	-7.16	19.73	46.11	4.14	11.21
	Chastre and Silva (2010)	-42.74	-10.14	-35.69	-3.19	-11.75	20.58	-32.28	0.29	-14.45	18.26	-82.22	-47.25	13.68	47.25	-44.46	-11.88
	Wei and Wu (2012)	11.08	-15.94	12.76	-13.04	19.21	-2.03	13.62	-11.88	18.43	-3.19	2.86	-29.86	28.18	14.20	31.76	21.16

The stress-strain curves for columns confined with CFRP were analysed for the models with the lowest error values (see Fig. 2). The lowest error of the W of the coupled models for CFRP have been compared with the experimental test and are presented in Table 6.

For specimen C1, the stress-axial strain curve of the model by Chastre and Silva (2010) coupled with equation (6) presents similar behaviour to the specimen. Regarding the stress-lateral strain curves, no model was representative of the behaviour of the experimental test. When analysing the error of W, the model with less error is the model by Spoelstra and Monti (1999) coupled with equation (3). Regarding the stress-axial strain curves of specimen C5, the models by Spoelstra and Monti (1999) coupled with equations (5) and (10) and by Chastre and Silva (2010) coupled with equations (2) and (10), represents the curve behaviour of the specimen. When analysing W, the error value of the model by Chastre and Silva (2010) coupled with equation (2) is the smallest value.

Table 6. Error of strain energy dissipation for specimens confined with CFRP.

Model	C1		C5		C20C1		C20C2	
	Equation	W	Equation	W	Equation	W	Equation	W
Spoelstra and Monti (1999)	(3)	3.61	(5)	-6.21	(4)	-8.62	(4)	-36.53
	(10)	-4.75	(10)	-20.84			(9)	17.57
Lam and Teng (2003a)	(5)	16.80	(9)	27.92	(10)	18.53	(4)	4.59
	(10)	5.60	(10)	-77.12			(5)	-21.61
Chastre and Silva (2010)	(3)	-13.09	(2)	-5.78	(4)	42.87	(4)	19.20
	(6)	25.66	(10)	-8.32	(10)	10.67	(5)	-18.31
Wei and Wu (2012)	(10)	51.44	(7)	20.47	(10)	27.11	(2)	-1.15
			(10)	-7.39			(4)	17.45

For specimens C20C1 and C20C2, the stress-axial strain behaviour of the model by Spoelstra and Monti (1999) coupled with equation (4) and with equations (4) and (9), represents well the behaviour of specimens C20C1 and C20C2, respectively. When analysing the error of W for specimen C20C1, it is noted that the error of the model by Spoelstra and Monti (1999) coupled with equation (4) is the smallest value. The analysis of the error of W for specimen C20C2 points out the model by Wei and Wu (2012) as the one with the smallest error value, but, as can be graphically observed, this model is not representative of the specimen behaviour. Regarding the stress-lateral strain of all specimens confined with CFRP, no model is sufficiently accurate in the prediction of the lateral strain curve of the specimens with exception of the experimental test C5.

The errors between numerical models and experimental tests, regarding f_{cc} and ε_{cc}, for columns with circular cross-section confined with GFRP are presented in Table 7.

Table 7. Error of model predictions compared to experimental results for columns confined with GFRP.

Specimen	Model	Equation (4)		Equation (5)		Equation (6)		Equation (7)		Equation (9)	
		f_{cc}	ε_{cc}	f_{cc}	ε_{cc}	f_{cc}	ε_{cc}	f_{cc}	ε_{cc}	f_{cc}	ε_{cc}
GE	Spoelstra and Monti (1999)	8.86	-69.28	6.29	-89.54	10.00	-60.78	-1.47	-162.09	18.28	-7.84
	Lam and Teng (2003a)	18.75	7.84	15.63	-1.96	20.00	11.76	5.21	-44.44	28.74	37.25
	Wei and Wu (2012)	27.26	33.99	25.12	30.72	28.14	35.29	18.02	20.92	34.24	45.10
	Jesus et al. (2018)	4.52	14.38	2.35	6.54	5.39	17.65	-4.69	-20.26	11.91	40.52
G1	Spoelstra and Monti (1999)	-12.92	-66.91	-15.92	-87.05	-11.79	-59.71	-24.97	-157.55	-2.53	-7.91
	Lam and Teng (2003a)	-2.53	15.11	-5.74	6.47	-1.27	18.71	-16.45	-25.18	7.62	40.29
	Wei and Wu (2012)	24.23	23.02	22.02	19.42	25.09	24.46	14.63	7.19	31.33	35.97
	Jesus et al. (2018)	-21.85	10.79	-24.42	1.44	-20.84	13.67	-32.48	-28.06	-13.03	38.85
G2	Spoelstra and Monti (1999)	-7.69	-31.76	-10.91	-48.07	-6.43	-25.75	-20.11	-104.72	4.13	16.31
	Lam and Teng (2003a)	2.61	13.73	-2.00	3.43	4.42	17.60	-17.42	-34.33	17.25	43.35
	Wei and Wu (2012)	29.52	33.05	26.47	29.61	30.72	34.76	16.24	17.17	39.33	45.92
	Jesus et al. (2018)	-4.21	33.05	-6.84	26.61	-3.21	35.62	-15.38	6.01	4.36	52.79
EE75C	Spoelstra and Monti (1999)	8.20	-167.27	5.53	-200.00	9.30	-154.55	-2.60	-319.09	17.96	-69.09
	Lam and Teng (2003a)	17.70	-41.82	14.29	-58.18	19.04	-35.45	2.74	-117.27	28.53	4.55
	Wei and Wu (2012)	27.12	-2.73	24.78	-8.18	28.03	-0.91	16.95	-24.55	34.62	15.45
	Jesus et al. (2018)	5.22	-26.36	2.98	-38.18	6.13	-20.91	-4.47	-78.18	12.77	11.82

The stress-strain curves for columns confined with GFRP were analysed, for the models with the lowest error values (see Fig. 3). The lowest errors of the W of the models for GFRP have been compared with the W of the specimens, and are presented in Table 8.

Table 8. Error of strain energy dissipation for specimens confined with GFRP.

Model	GE		G1		G2		EE75C	
	Equation	W	Equation	W	Equation	W	Equation	W
Spoelstra and Monti (1999)	(7)	-122.61	(9)	-11.87	(9)	17.10	(7)	-291.07
	(9)	8.80					(9)	-43.93
Lam and Teng (2003a)	(5)	15.40	(5)	4.39	(5)	5.46	(7)	-75.17
	(7)	-25.28	(6)	19.51			(9)	30.50
Wei and Wu (2012)	(7)	42.45	(7)	29.95	(7)	39.29	(6)	27.30
							(7)	4.21
Jesus et al. (2018)	(7)	-2.07	(5)	-14.22	(7)	9.06	(7)	-60.70
			(9)	35.34			(9)	24.93

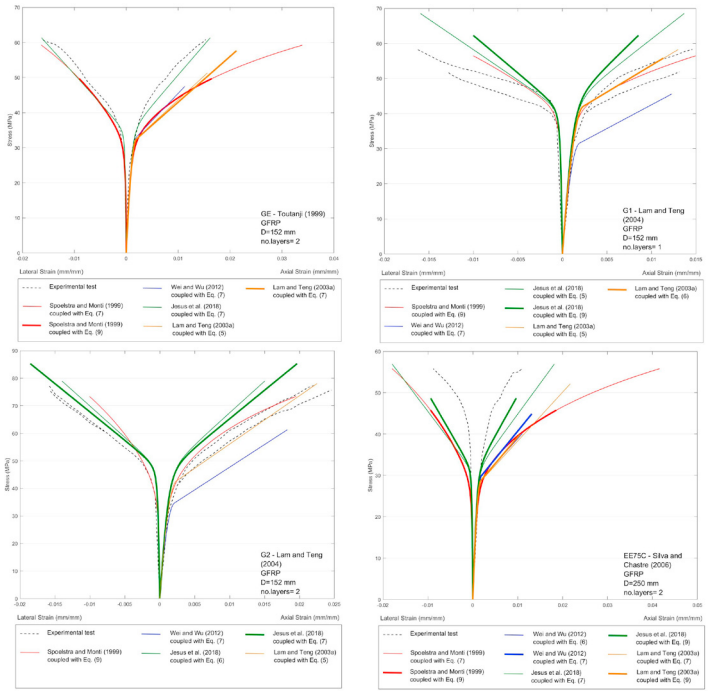

Fig. 3. Comparison of the numerical stress-strain curves with the experimental data for columns confined with GFRP.

In stress-axial and lateral strain response of specimen GE, the model by Jesus et al. (2018) coupled with equation (7) is representative of the behaviour of the experimental test. The analysis of the W for specimen GE shown that the model by Jesus et al. (2018) presents the smallest value of error, in accordance to the graphic visualization. Regarding the specimen G1, the stress-axial strain response of the models by Lam and Teng (2003a) and by Spoelstra and Monti (1999), coupled with equations (5) and (6) and equation (9), respectively, present the closest response to the specimen behaviour. For the stress-lateral strain response, no model is able to predict the curve behaviour of the specimen. In concern to the analysis of W, the model by Lam and Teng (2003a) coupled with equation (5) presents the smaller error in comparison with the experimental tests.

For specimen G2, the stress-axial strain curve of the models by Lam and Teng (2003a) coupled with equation (5) and by Spoelstra and Monti (1999) coupled with equation (9) represent the behaviour of the specimen. The stress-lateral strain behaviour presented by the model of Jesus et al. (2018) coupled with equation (7) present the better fit with the experimental tests. Regarding the error of W, the model by Lam and Teng (2003a) coupled with equation (5) presents the smaller value. In relation to specimen EE75C, for both stress-axial strain and stress-lateral strain curves, no model is able to predict the behaviour of the experimental test. In accordance, the error values of W are high.

4. Conclusions

The accuracy of existing models of confined concrete coupled with different proposals for the prediction of the FRP failure strain was assessed. The models by Spoelstra and Monti (1999) and by Silva Lobo et al. (2018) coupled with equations (1), (5) and (7) present the most accurate stress-axial strain curves in comparison with the experimental tests considered for columns confined with AFRP. The stress-lateral strain response of specimens with AFRP were not accurately predicted by the models coupled with any of the considered equations in half of the tests. Regarding the remaining cases, the results were adequately represented by the models by Silva Lobo et al. (2018) coupled with equations (1), (4) and (7), and by Spoelstra and Monti (1999) coupled with equations (1) and (9). Regarding the prediction of W, the smallest errors were obtained with the model by Silva Lobo et al. (2018) coupled with equation (7).

The models by Spoelstra and Monti (1999) coupled with equations (4), (5), (9) and (10) and by Chastre and Silva (2010) coupled with equations (2), (6) and (10) delivered the most accurate stress-axial strain response in comparison with the experimental tests for columns confined with CFRP. In almost all specimens confined with CFRP, the models were not capable of predicting the stress-lateral strain curve. The error in W was smaller for the model by Spoelstra and Monti (1999) coupled with equation (3).

Regarding the specimens confined with GFRP, the models by Spoelstra and Monti (1999) coupled with equation (9), by Lam and Teng (2003a) coupled with equation (5) and by Jesus et al. (2018) coupled with equation (7) presented the most representative stress-axial strain response. In most specimens, the stress-lateral strain curve was not represented by the models. Regarding W, the models by Lam and Teng (2003a) coupled with equation (5) and Jesus et al. (2018) coupled with equation (7) presented the smaller value of error in comparison the experimental test.

The use of equations (5) and (7) allowed to obtain better results in 40 % of the cases, and the use of equations (1) and (9) allowed to obtain better results in 30% of the cases. This was observed when the equations were coupled with the models by Spoelstra and Monti (1999), Silva Lobo et al. (2018) and Jesus et al. (2018).

References

Arabshahi, A., Gharaei-Moghaddam, N., & Tavakkolizadeh, M. (2020). Development of applicable design models for concrete columns confined with aramid fiber reinforced polymer using Multi-Expression Programming. Structures, 23, 225-244.

Benzaid, R., Mesbah, H., & Chikh, N. E. (2010). FRP-confined concrete cylinders: axial compression experiments and strength model. Journal of Reinforced plastics and composites, 29(16), 2469-2488.

Berthet, J. F., Ferrier, E., & Hamelin, P. (2005). Compressive behavior of concrete externally confined by composite jackets. Part A: experimental study. Construction and building materials, 19(3), 223-232.

Chastre, C., & Silva, M. A. (2010). Monotonic axial behavior and modelling of RC circular columns confined with CFRP. Engineering Structures, 32(8), 2268-2277.

Dai, J. G., Bai, Y. L., & Teng, J. G. (2011). Behavior and modeling of concrete confined with FRP composites of large deformability. Journal of composites for construction, 15(6), 963-973.

Ilki, A., Kumbasar, N., & Koc, V. (2004). Low strength concrete members externally confined with FRP sheets. Structural Engineering and Mechanics, 18(2), 167-194.

Jesus, M., Silva Lobo, P., & Faustino, P. (2018). Design models for circular and square RC columns confined with GFRP sheets under axial compression. Composites Part B: Engineering, 141, 60-69.

Lam, L., & Teng, J. (2003a). Design-oriented stress–strain model for FRP-confined concrete. Construction and building materials, 17(6-7), 471-489.

Lam, L., & Teng, J. (2003b). Design-oriented stress-strain model for FRP-confined concrete in rectangular columns. Journal of reinforced plastics and composites, 22(13), 1149-1186.

Lam, L., & Teng, J. (2004). Ultimate condition of fiber reinforced polymer-confined concrete. Journal of Composites for Construction, 8(6), 539-548.

Mander, J., Priestley, M., & Park, R. (1988). Theoretical stress-strain model for confined concrete. Journal of structural engineering, 114(8), 1804-1826.

Manfredi G, Realfonzo R. (2001). Models of concrete confined by fiber composites. In: Proc., 5th Annual Symp. on Fibre-Reinforced-Plastic Reinforced for Concrete Structures. Thomas Telford; 2001:865–74.

Matthys, S., Toutanji, H., Audenaert, K., & Taerwe, L. (2005). Axial load behavior of large-scale columns confined with fiber-reinforced polymer composites. ACI Structural Journal, 102(2), 258.

Ozbakkaloglu, T., & Lim, J. (2013). Axial compressive behavior of FRP-confined concrete: Experimental test database and a new design-oriented model. Composites Part B: Engineering, 55, 607-634.

Popovics, S. (1973). A numerical approach to the complete stress-strain curve of concrete. Cement and concrete research, 3(5), 583-599.

Richard, R., & Abbott, B. (1975). Versatile elastic-plastic stress-strain formula. Journal of the Engineering Mechanics Division, 101(4), 511-515.

Silva, M., & Chastre, C. (2006). Size and relative stiffness effects on compressive failure of concrete columns wrapped with glass FRP. Journal of Materials in Civil Engineering, 18(3), 334-342.

Silva Lobo, P., Faustino, P., Jesus, M., & Marreiros, R. (2018). Design model of concrete for circular columns confined with AFRP. Composite Structures, 200, 69-78.

Spoelstra, M., & Monti, G. (1999). FRP-confined concrete model. Journal of composites for construction, 3(3), 143-150.

Toutanji, H. (1999). Stress-strain characteristics of concrete columns externally confined with advanced fiber composite sheets. Materials Journal, 96(3), 397-404.

Toutanji, H., Han, M., Gilbert, J., & Matthys, S. (2010). Behavior of large-scale rectangular columns confined with FRP composites. Journal of Composites for Construction, 14(1), 62-71.

Vincent, T., & Ozbakkaloglu, T. (2013). Influence of fiber orientation and specimen end condition on axial compressive behavior of FRP-confined concrete. Construction and Building materials, 47, 814-826.

Wei, Y., & Wu, Y. (2012). Unified stress–strain model of concrete for FRP-confined columns. Construction and Building Materials, 26(1), 381-392.

Wu, G., Wu, Z., Lu, Z., & Ando, Y. (2008). Structural performance of concrete confined with hybrid FRP composites. Journal of reinforced plastics and composites, 27(12), 1323-1348.